Frontiers in Bioscience Landmark

Front. Biosci. (Landmark Ed) **2026**; 31(3): 48371
https://doi.org/10.31083/FBL48371

Original Research

TNFRSF21 Orchestrates Epithelial Keratinization and Tight Junction Integrity in Periodontitis-Associated Oral Mucosal Repair

Wenhao Zhang[1,2,†], Yulong Zhang[1,†], Zhongxuan Sun[1], Siyu Jin[1], Bin Liu[1], Fei Xu[1], Yutong Lu[1], Ying Yang[3], Mingyue Wu[1,*], Wansu Sun[1], Hengguo Zhang[1,*]

[1]College & Hospital of Stomatology, Anhui Medical University, Anhui Provincial Key Laboratory of Oral Diseases Research, 230032 Hefei, Anhui, China
[2]Stomatology Hospital, School of Stomatology, Zhejiang University School of Medicine, Zhejiang Provincial Clinical Research Center for Oral Diseases, Key Laboratory of Oral Biomedical Research of Zhejiang Province, Engineering Research Center of Oral Biomaterials and Devices of Zhejiang Province, 310000 Hangzhou, Zhejiang, China
[3]School of Pharmaceutical Sciences, Anhui Medical University, 230032 Hefei, Anhui, China
*Correspondence: wumingyue321@126.com (Mingyue Wu); zhanghengguo@ahmu.edu.cn (Hengguo Zhang)
[†]These authors contributed equally.
Academic Editor: Eun Sook Hwang
Submitted: 19 November 2025 Revised: 6 January 2026 Accepted: 27 January 2026 Published: 17 March 2026

Abstract

Background: The progression of periodontitis is accompanied by destruction of keratinized epithelium, while members of the tumor necrosis factor receptor superfamily (TNFRSF) play critical roles in epithelial repair. This study aimed to elucidate the role of TNFRSF in the pathogenesis and progression of periodontitis. Furthermore, we investigated the mechanisms underlying the repair of epithelial keratinization, with the ultimate aim of translating these insights into clinical therapeutic applications. **Methods**: Single-cell RNA sequencing was used to investigate the TNFRSF expression profiles in the gingival epithelium of patients with severe periodontitis. Gingival tissues were collected from healthy individuals and those with periodontitis. An *in vitro* model was also established using retinoic acid to inhibit keratinization and BMS493 to promote keratinization. Bulk RNA sequencing was performed to further substantiate the model and validated the findings by gene knockdown and overexpression experiments. Protein–protein interaction (PPI) analysis and immunoprecipitation identified key protein interactions. In addition, a *TNFRSF21* overexpression plasmid and a full-thickness dorsal skin wound mouse model were used to confirm regulatory processes during keratinization. **Results**: *TNFRSF21* expression, along with epithelial keratinization-related genes were significantly reduced in clinical periodontitis tissues. However, *TNFRSF21* increased significantly during epithelial repair following initial periodontal therapy for severe periodontitis, particularly in proliferative keratinocytes and basal layer cells. An *in vitro* keratinization model revealed that *TNFRSF21*, Keratin 8 (*KRT8*), and *KRT18*, were downregulated during the inhibition of keratinization and upregulated during its promotion. Importantly, the expression levels of *KRT8*, *KRT18*, and *Claudin-1* were consistently downregulated in the *TNFRSF21* knockdown group and upregulated in the *TNFRSF21* overexpression group. Single-cell RNA sequencing combined with PPI analysis revealed a significant interaction between TNFRSF21 and amyloid precursor protein (APP). This was validated by STRING database analysis and immunoprecipitation. Mice treated with *TNFRSF21* overexpression plasmids showed accelerated wound healing and increased keratin expression on dorsal skin. **Conclusions**: Our findings indicate that *TNFRSF21* is a pivotal regulator of epithelial keratinization and tight junction integrity in oral epithelial keratinocytes. Targeting *TNFRSF21* may represent a novel therapeutic strategy to restore oral epithelial function.

Keywords: periodontitis; epithelium; keratins; TNFRSF21 protein; single-cell analysis

1. Introduction

Periodontitis is a major global health burden affecting billions of people. It is characterized by symptoms ranging from gingival bleeding and tooth mobility to severe tooth loss [1,2]. Current clinical interventions for periodontitis primarily target the suppression of inflammation, but fail to restore the original periodontal architecture. The mechanistic understanding of disease progression is thus imperative for the development of regenerative therapeutic paradigms [3,4].

Healthy gingiva is able to maintain normal keratinized epithelial attachment [5]. In periodontitis, the loss of gingival keratinization leads to gingival recession and clinical loss of attachment [6]. The standard treatment is periodontal debridement and appropriate application of mouthwash, such as those containing chlorhexidine. This removes subgingival calculus and plaque, thereby reducing gingival irritation and promoting epithelial reattachment. The adjunctive use of antimicrobial mouth rinses is supported by *in vitro* evidence demonstrating the antibacterial efficacy of agents like chlorhexidine against oral pathogens [7,8]. Importantly, oral epithelial keratinocytes show upregulated expression of epithelial keratinization-related genes (KRTs) and exhibit high proliferative and differentiation capacities that drive tissue regeneration [9]. These cells maintain the

oral mucosal barrier and produce keratin, which is essential for epithelial protection [10].

The tumor necrosis factor receptor superfamily (TNFRSF) comprises diverse transmembrane proteins that are prominently expressed on cell surfaces [11]. These receptors orchestrate various physiological and pathological processes, including cell signaling transduction, immune modulation, cell proliferation, differentiation, and apoptosis [12]. TNFRSF-ligand interactions are critical in immune regulation and cancer therapy [12,13]. For instance, the binding of soluble Fas ligand (sFasL) to death receptor 5 exacerbates autoantibody-induced arthritis [14]. Such interactions modulate autoimmune responses and confer dual effects in cancer by either fostering tumor cell proliferation/survival, or triggering cancer cell apoptosis [15–17]. However, potential links between TNFRSF mechanisms and the development of periodontitis or gingival epithelium keratinization remain unexplored.

In the present study, our aim was to elucidate the role of TNFRSF in periodontitis-associated disorders of keratinization. Additionally, we explored the underlying mechanism for the repair of epithelial keratinization, with the goal of translating these findings into clinical periodontal therapy. Our hypothesis is that TNFRSF plays a pivotal role in maintaining gingival epithelial homeostasis, and that dysfunction of TNFRSF is a key mechanism underlying the impairment of keratinization and poor healing observed in periodontitis. We first evaluated post-treatment epithelial changes in patient samples, then investigated the mechanism of epithelial keratinization injury at the cellular level. Subsequently, we validated the findings in an animal model, with the ultimate aim of translating the results into the clinic for patient benefit. Our study found a novel molecular mechanism involving *TNFRSF21* and which appears to underlie defective keratinization in periodontal tissues and keratinocyte differentiation. Overexpression of *TNFRSF21* promotes the expression of keratin by oral epithelial keratinocytes, leading to wound keratinization and suggesting that it may be a promising therapeutic target. We also developed an *in vitro* keratinization gradient model using small molecule drugs, offering a new tool to study the loss of epithelial keratinization. These findings provide a new perspective on the pathogenesis of periodontitis and suggest that *TNFRSF21*-targeted strategies could be used to treat impaired keratinization in periodontal disease.

2. Materials and Methods

2.1 Cell Culture

Human oral keratinocytes (HOKs) were purchased from Shanghai QuiCell Biotechnology Co., Ltd. The item number is QuiCell-Y1694. These were STR-certified and free of mycoplasma. Following resuscitation in cell culture flasks, the cells were incubated at 37 °C with 5% CO_2 for 3–4 hours to stabilize their condition. The complete culture medium consisted of DMEM (11965092, Thermo Fisher Scientific, Waltham, MA, USA) supplemented with 10% fetal bovine serum, 100 U/mL penicillin, and 0.1 mg/mL streptomycin. Upon reaching 70% confluency, the cells were detached using 0.25% trypsin and passaged at a 1:2 ratio [18].

2.2 Inhibition and Promotion Models of In Vitro Keratinization

Resuscitated HOKs were seeded into six-well culture plates, and 2 mL of complete medium (DMEM supplemented with 10% fetal bovine serum, penicillin, and streptomycin) was added to each well. The cells were cultured in an incubator at 37 °C and 5% CO_2 until they reached 70%–80% confluence. Treatment groups were exposed to 0, 1, and 10 µM concentrations of retinoic acid (RA), or 0, 100, and 500 nM concentrations of BMS493. The drug-containing medium was replaced every two days to ensure stable drug concentrations. On day 9 of culture, cell samples were collected for experiments, including Western blotting to detect changes in the expression of keratinization-related markers.

2.3 Transfection of Small Interfering RNAs (siRNAs) and Plasmids

An siRNA that targets *TNFRSF21* was designed and synthesized by TsingKe Biological (Beijing, China). The adenovirus vector GV315 containing *TNFRSF21* (NM_014452.5) was purchased from TsingKe Biological (Beijing, China). Transfection was performed using Lipofectamine 2000 (TsingKe Biological) in accordance with the manufacturer's instructions. All sequence details are provided in **Supplementary Table 1**.

2.4 Animal Experiment

All animal work was performed in accordance with the ARRIVE guidelines 2.0. The experimental procedures were approved by the Laboratory Animal Care and Use Committee at Anhui Medical University (Approval No. LLSC20232087). Eight C57BL/6 mice aged 8 months were randomly and equally divided into two groups via a simple randomization method using a random number generator. The first group (negative control) received an empty vector plasmid (Vector), while the second group was treated with a plasmid for the overexpression of *TNFRSF21* (OE-TNFRSF21). Under surgical anesthesia induced by 2% sodium pentobarbital (50 mg/kg), all mice underwent full-thickness excisional wounds on their dorsal sides. Following hair removal on the back, two 6-mm full-thickness wounds were made along the midline of the back of each mouse using a sterile biopsy punch. Immediately after wounding, the mice were given multiple subcutaneous injections of either the empty vector or the OE-TNFRSF21 plasmid (four injections per wound site), with each wound receiving a single treatment. Additionally, by adding the opioid tramadol (0.1 mg/mL) to the drinking water to al-

leviate pain related to wounds [19]. On day 9 postoperatively, mice were euthanized via cervical dislocation following induction with 5% isoflurane anesthesia. The dorsal wound tissues were harvested for histological examination and fixed in a 4% paraformaldehyde solution, along with visceral organs, including the heart, liver, spleen, lungs, and kidneys. Subsequently, quantitative histomorphometric analysis was conducted on these tissues to evaluate the progress of wound healing and the overall systemic biocompatibility associated with plasmid therapy.

2.5 Analysis of Single-Cell RNA-Seq and Bulk RNA-Seq

Patients were classified based on clinical and radiographic (X-ray) criteria. Periodontal tissues were collected during tooth extraction or ridge repair, placed in sterile PBS tubes, and transported to the laboratory within 10 minutes for single-cell preparation and RNA sequencing. The periodontal therapy (PDT) patient group (n = 3) showed minimal gingival inflammation after treatment, but had severe clinical attachment and bone loss (>60%) [20]. Single-cell RNA sequencing (scRNA-seq) was performed by NovelBio Bio-Pharm Technology Co., Ltd, employing the NovelBrain Cloud Analysis Platform as described previously [21,22]. scRNA-seq data were obtained from NCBI GEO (GSE171213). Raw sequencing data were processed with Cell Ranger (v7.1.0, 10x Genomics, Pleasanton, CA, USA) for alignment, barcode assignment, and unique molecular identifier (UMI) counting. Rigorous quality control (QC) steps were applied, with cells expressing <200 genes, cells with >20% mitochondrial reads, and potential doublets identified via the DoubletFinder algorithm (v2.0.3, Christopher S. McGinnis, University of California, San Francisco, CA, USA) excluded from downstream analyses. Cell normalization and regression analysis were performed using the Seurat package (v2.3.4, Satija Lab, New York Genome Center, New York, NY, USA) based on UMI counts and the proportion of mitochondrial genes, resulting in scaled expression data [23]. To mitigate potential batch effects that could compromise analytical accuracy, the Harmony package was employed using the top 3000 highly variable genes under default parameters [24]. Unsupervised clustering was conducted using a graph-based algorithm with a resolution of 0.8, based on the top 10 principal components obtained from principal component analysis (PCA). Marker genes were identified using the FindAllMarkers function with the Wilcoxon rank-sum test, applying the following criteria: log-fold change (lnFC) >0.25, p-value < 0.05, and minimum expression percentage (min.pct) >0.1 [20]. After QC, a total of 622 single cells were retained. Clustering and dimensionality reduction were conducted using Seurat with t-Distributed Stochastic Neighbor Embedding (t-SNE) [25]. Ligand-receptor interaction analysis was performed using the CellPhoneDB toolkit to construct an interaction network of TNFRSF members and their ligands in oral epithelial cells. The String database (v12.0, STRING Consortium (SIB), Geneva, Switzerland) was used for visual analysis [26]. Bulk RNA-seq analysis was conducted on three samples from each group: negative control (NC), keratinization inhibition induced by RA treatment (10 μM), and keratinization promotion induced by BMS493 treatment (500 nM). Raw sequencing reads were aligned to the human genome (GRCh38) using STAR (v2.7.10a, Alexander Dobin, Cold Spring Harbor Laboratory, NY, USA). Differential expression analysis was performed using DESeq2 (v1.38.3, Simon Anders, European Molecular Biology Laboratory, Heidelberg, Germany) [27]. Gene Ontology (GO) and Kyoto Encyclopedia of Genes and Genomes (KEGG) enrichment analyses were conducted using clusterProfiler (v4.8.1, Guangchuang Yu, Southern Medical University, Guangzhou, Guangdong, China) [28]. Differentially expressed genes (DEGs) were identified using a threshold of absolute $\log_2$-fold change >1 and an adjusted p-value (FDR) < 0.05.

2.6 Protein Extraction and Western Blotting

Gingival tissues collected from clinical samples of healthy volunteers or periodontitis patients were homogenized in RIPA lysis buffer (1×, P0013B, Beyotime Biotechnology, Shanghai, China) for protein extraction. The lysates were incubated on ice for 20 min with agitation, followed by centrifugation at 13,000 rpm and 4 °C for 10 min. The supernatant was transferred to a new 1.5 mL microcentrifuge tube, mixed 1:1 with 2× SDS-PAGE loading buffer (P0015B, Beyotime, Shanghai, China) containing protease and phosphatase inhibitors, boiled at 95 °C for 10 min, and stored at –20 °C or directly subjected to Western blot analysis. Protein samples were separated on a Bis-Tris Gel (12%, 20214ES08, Yeasen Biotechnology, Shanghai, China), and then transferred to a 0.45 μm pore size PVDF membrane (0.45 μm, IPVH00010, Merck, Darmstadt, Germany) in ice-cold transfer buffer for 2 h. After blocking with 5% non-fat milk for 1 h at room temperature, the membrane was incubated overnight at 4 °C with the primary antibody. After washing four times with TBST (Tris-buffered saline with Tween 20) for 7 min, the membrane was incubated with HRP-conjugated secondary antibodies (1:5000, SA00001-1/SA00001-2, Proteintech, Rosemont, IL, USA) for 1 h at room temperature, then washed four times with TBST (5 min each). The membrane was imaged using a CCD camera to visualize the immunoreactive bands following enhancement with chemiluminescence (Tanon-5200, Tanon Science & Technology Co., Ltd., Shanghai, China). GAPDH (Glyceraldehyde-3-Phosphate Dehydrogenase) was utilized as the housekeeping gene. Densitometric analysis was performed on all bands using GAPDH as the reference for normalization.

2.7 Immunoprecipitation (IP)

Protein A/G beads (50 μL per reaction, HY-K0202, MedChemExpress, Monmouth Junction, NJ, USA) were

washed with an appropriate amount of IP buffer, then centrifuged, and the supernatant discarded. TNFRSF21 or IgG antibody (2 µg) was added before incubation for 4–6 h at 4 °C to couple the antibody with the beads. The supernatant from lysed HOKs was then collected, and 100 µL was taken as the Input group. The remaining cell lysate was added to the pre-treated beads and incubated at 4 °C overnight to allow the TNFRSF21 protein to bind with the specific antibody. Next, the beads were washed three times with lysis buffer to remove unbound proteins. Loading buffer (5×) was subsequently added and the sample heated at 95 °C for 15 minutes for analysis by Western blotting, or storage at –20 °C. Western blotting was performed using standard protocols, with the antibodies listed in **Supplementary Table 1**.

2.8 Hematoxylin and Eosin (H&E) Staining

Tissue sections (4 µm) were subjected to H&E staining using standardized protocols. Briefly, deparaffinized sections were stained with Mayer's hematoxylin (4 min) and then differentiated (1% acid ethanol, 3 sec), blued (0.2% ammonia water), and counterstained with eosin Y (3 min). After dehydration and mounting, the slides were imaged using a Nikon Eclipse E100 microscope (Nikon Eclipse E100, Nikon Instruments Inc., Tokyo, Japan).

2.9 Immunofluorescence Staining of Paraffin-Embedded Tissues

Tissue sections were deparaffinized in xylene (2 × 15 min) and then rehydrated through a graded ethanol series (100%, 100%, 85%, and 75% for 5 min each) followed by rinsing in distilled water. Antigen retrieval was performed in citrate buffer (10 mM, pH 6.0) using microwave heating (95 °C, 20 min). After cooling, slides were washed in PBS (3 × 5 min).

Tissue sections were encircled with a hydrophobic barrier, treated with an autofluorescence quencher (G1221, Servicebio, Wuhan, Hubei, China) for 5 min, and rinsed under running water (10 min). Non-specific binding was blocked with 3% BSA/PBS (30 min, RT). Primary antibodies (diluted in PBS) were applied and incubated overnight at 4 °C in a humidified chamber. After PBS washes (3 × 5 min), fluorophore-conjugated and species-matched secondary antibodies (Servicebio, Wuhan, Hubei, China) were applied (50 min, RT, dark). Nuclei were counterstained with DAPI (1 µg/mL, 10 min, dark). Sections were then mounted with anti-fade medium (Servicebio, G1401) and imaged using a fluorescence microscope (Nikon Eclipse Ni-E, Tokyo, Japan) with standard filter sets (DAPI: Ex 330–380 nm/Em 420 nm; FITC: Ex 465–495 nm/Em 515–555 nm; Cy3: Ex 510–560 nm/Em 590 nm).

3. Results

3.1 TNFRSF21 Expression in Oral Epithelial Cells

To investigate whether TNFRSF regulates the healing process after treatment for severe periodontitis, we analyzed single-cell RNAseq of gingival epithelial tissues collected after initial PDT [20]. t-SNE cluster analysis performed on the scRNA-seq data of oral epithelial cells revealed 7 distinct cell clusters (Fig. 1A). The differentiation trajectory was analyzed and visualized with partition-based graph abstraction (PAGA) (Fig. 1B). KEGG enrichment analysis revealed significant enrichment of the TNF signaling pathway within the Basal_V and Pro_KC cell clusters. In addition, signaling pathways related to tight junctions, inflammatory regulation, and interaction with extracellular mechanisms were also significantly enriched (Fig. 1C). Subsequently, we aggregated the expression data of TNFRSF across all cell clusters and observed that *TNFRSF21* was prominently expressed in each cluster. This consistent expression pattern indicates that *TNFRSF21* functions as a pivotal marker in modulating the healing processes of periodontitis (Fig. 1D).

3.2 Hypokeratinization in Periodontitis is Associated With the Expression of TNFRSF21

To further examine specific gene expression in periodontal epithelial tissues, we compared the expression of *TNFRSF21* and KRTs between individuals with periodontitis and healthy controls. The expression levels of both *TNFRSF21* and KRTs were found to be significantly reduced in the periodontitis group compared to the control group (Fig. 2A). Subsequently, we established an *in vitro* concentration gradient model for inhibiting and promoting keratinization in HOK cells using RA, a small molecule drug, and its inhibitor BMS493, respectively [29–31]. This model was designed to simulate the processes of incomplete keratinization in epithelial tissues during the onset of periodontitis, and of re-keratinization following treatment and recovery. Western blot analysis confirmed that expression levels for *TNFRSF21* and KRTs (including *KRT8* and *KRT18*) were significantly reduced in the keratinization inhibition group (RA), whereas they were significantly increased in the keratinization promotion group (BMS493; Fig. 2B). Differential gene analysis of bulk RNA sequencing showed that RA treatment reduced the expression of keratin proteins such as *KRT9*, *KRT16*, and *KRT17*, while increasing the expression of chemokines like C-C Motif Chemokine Ligand 2 (*CCL2*). Furthermore, bulk RNA sequencing data revealed excellent intra-group homogeneity and clear inter-group separation across the NC, RA, and BMS493 groups (Fig. 2C). Gene Ontology (GO) functional enrichment analysis revealed the DEGs were significantly correlated with cell differentiation, immune regulation, epithelial migration, and keratinization (Fig. 2D). These findings imply that epithelial regeneration, reduction of inflam-

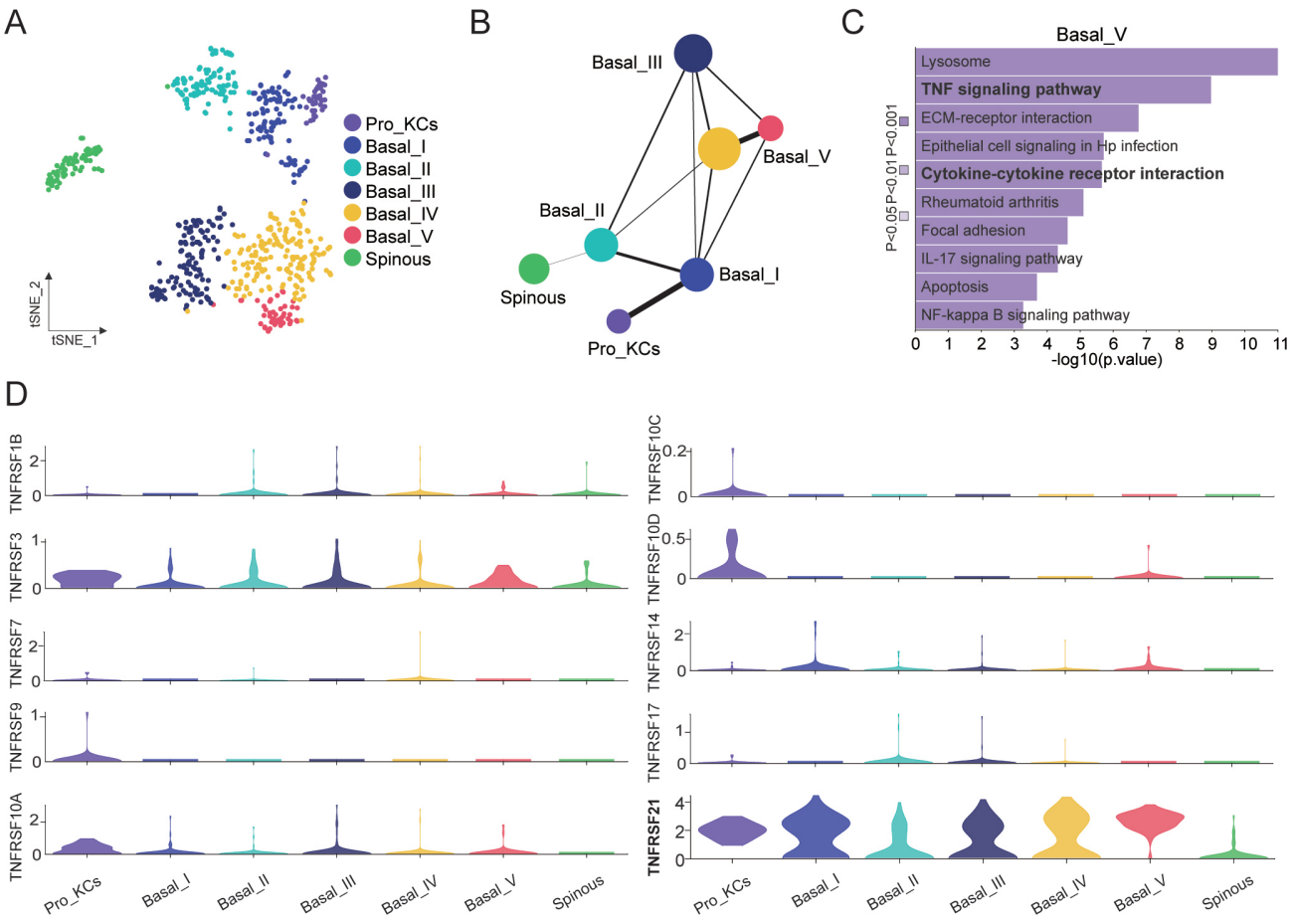

Fig. 1. Tumor necrosis factor receptor superfamily 21 (TNFRSF21) is a key molecule during periodontal regeneration and repair. (A) The main cell types present in the gingival epithelium after periodontal treatment were identified by the Seurat R package and visualized by t-Distributed Stochastic Neighbor Embedding (t-SNE). (B) Partition-based graph abstraction (PAGA) was employed to analyze and visualize the differentiation trajectories. (C) Kyoto Encyclopedia of Genes and Genomes (KEGG) enrichment analysis of Basal_V and Pro_KCs showed significant activation of the TNF signaling pathway. (D) Violin plot illustrating the expression levels of selected members of the TNFRSF family during the periodontitis healing process.

mation, and the critical regulatory role of keratinization are integral to both the pathogenesis of periodontitis and its therapeutic recovery.

3.3 Expression of TNFRSF21 in Oral Epithelial Cells Affects Keratinization

To further investigate the potential regulatory role of *TNFRSF21*, we employed gene knockdown and overexpression techniques to suppress and enhance its expression. Validation of the knockdown efficiency revealed markedly decreased *TNFRSF21* protein expression (Fig. 3A). We also examined alterations in the expression levels of target KRTs, including *KRT8*, *KRT18*, and *Claudin-1* (Fig. 3B). Subsequently, we constructed a plasmid for *TNFRSF21* overexpression and transfected it into HOK cells. This resulted in increased expression of *TNFRSF21*, as well as increased expression levels of *KRT8*, *KRT18*, and *Claudin-1* (Fig. 3C). Together, these findings support a regulatory role of *TNFRSF21* in keratin expression by HOK cells.

3.4 TNFRSF21 in Oral Epithelial Cells Specifically Binds to APP

TNFRSF is a class of cell surface receptor that typically mediates physiological functions upon binding to its ligands [12]. We next investigated interactions between the TNFRSF family and their ligands during treatment for periodontitis and subsequent healing. Through protein–protein interaction (PPI) analysis of scRNA-seq data (Fig. 4A), we identified a significant interaction between *TNFRSF21* and amyloid precursor protein (*APP*). Further validation via STRING database analysis of DEGs confirmed this interaction (Fig. 4B). Additionally, an immunoprecipitation (IP) assay provided direct evidence for the interaction between *TNFRSF21* and *APP* in HOK cells (Fig. 4C). These observations confirm the strong interaction between *TNFRSF21* and its ligand *APP* throughout the periodontitis recovery phase. Moreover, we speculate that the complex formation between *TNFRSF21* and *APP* may play a synergistic role in modulating the functions of oral epithelial keratinocytes.

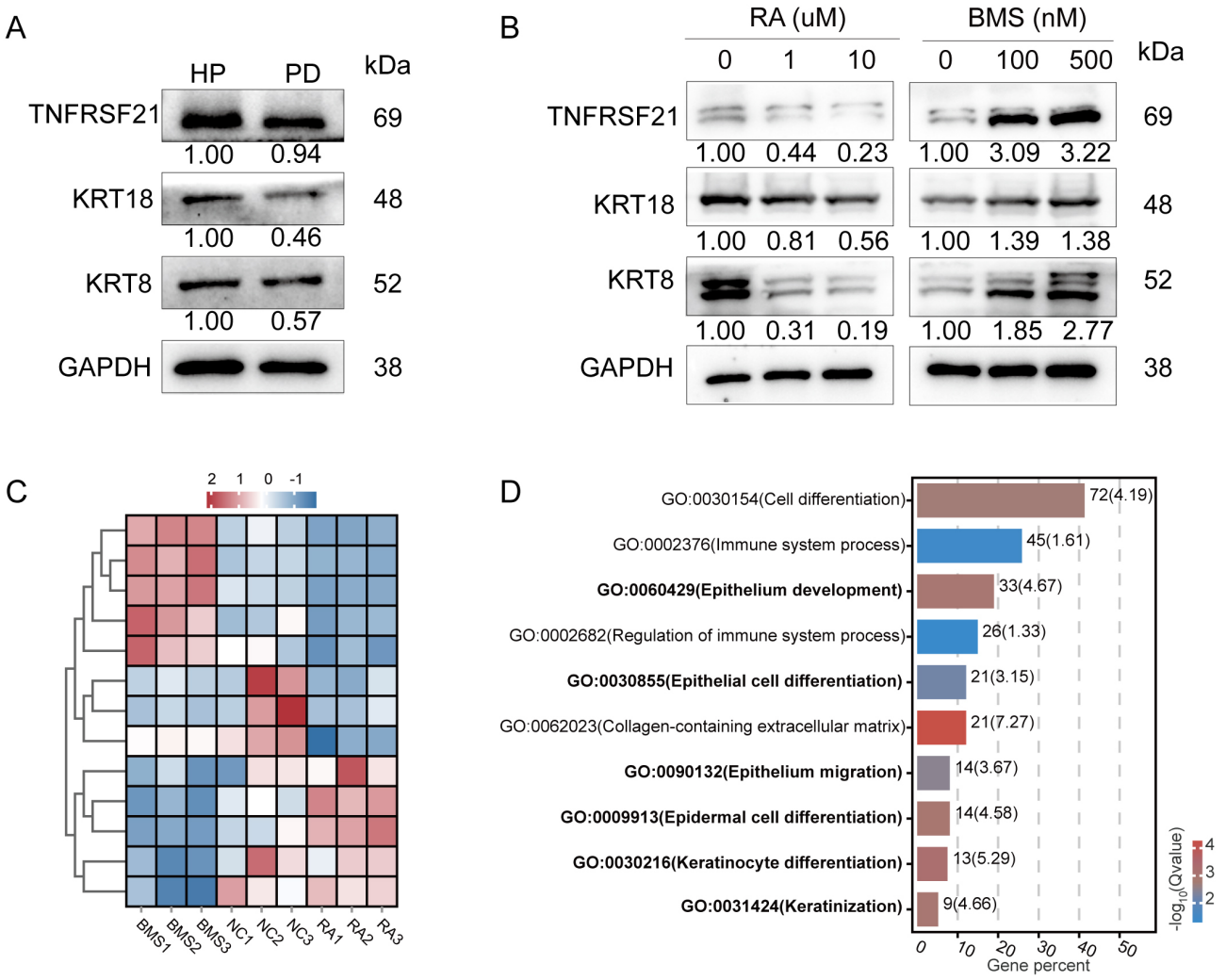

Fig. 2. Changes in TNFRSF21 expression during the keratinization process, as revealed by the *in vitro* keratinization induction model. (A) Western blot analysis showed a significant reduction in the expression levels of keratin and TNFRSF21 in the gingival epithelial tissues of periodontitis patients (PD) compared to healthy controls (HP). (B) *In vitro* models showed decreased TNFRSF21 and keratin expression in the keratinization inhibition group (treated with retinoic acid (RA)), and increased expression in the keratinization promotion group (treated with BMS493). (C) Bulk RNA sequencing revealed high intra-group consistency and clear segregation between the negative control (NC), RA, and BMS493 groups. (D) GO enrichment analysis of differentially expressed genes identified by bulk-RNA sequencing.

3.5 TNFRSF21 Promotes Keratinized Wound Healing

We next conducted animal experiments to further investigate the role of *TNFRSF21* in promoting keratinization and wound healing. Using a puncher, we created a 6-mm diameter wound on the back of C57BL/6 mice and subsequently injected plasmids into the wound site that contained either an empty vector, or a vector overexpressing *TNFRSF21*. Wound conditions were monitored and documented on days 1, 3, 5, 7, and 9 post-injection (Fig. 5A). On day 9, a biopsy of the wound tissue was performed, followed by hematoxylin and eosin (H&E) staining and immunofluorescence analysis. Our findings revealed that the plasmid overexpression group had approached full wound closure by day 9. In contrast, the control group still presented with a substantial wound area at day 9. Additionally, mice treated with the *TNFRSF21*-overexpressing plasmid showed enhanced wound healing, characterized by a more rapid decrease in wound size and elevated keratin expression levels compared to the control group (Fig. 5B,C,E). Systemic effects of the overexpressing plasmid on the heart, liver, spleen, lung, and kidney tissues were also investigated by H&E staining, but no evidence of toxicity was observed (Fig. 5D).

4. Discussion

Periodontitis is a chronic inflammatory disease that presents significant global health challenges. It profoundly compromises oral health and has been linked to systemic

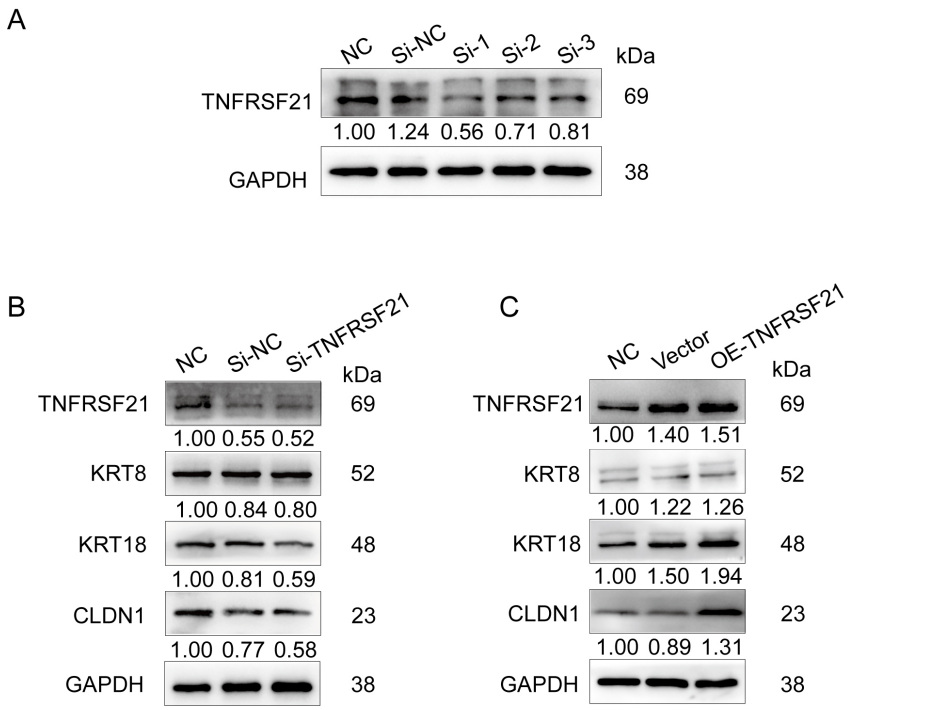

Fig. 3. Knockdown and overexpression of TNFRSF21 demonstrate its regulatory role during keratinization. (A) Verification of TNFRSF21 knockdown efficiency with siRNA. (B) Knockdown of TNFRSF21 reduced the expression of KRTs. (C) Overexpression of TNFRSF21 significantly increased the expression of KRTs. KRTs, keratinization-related genes.

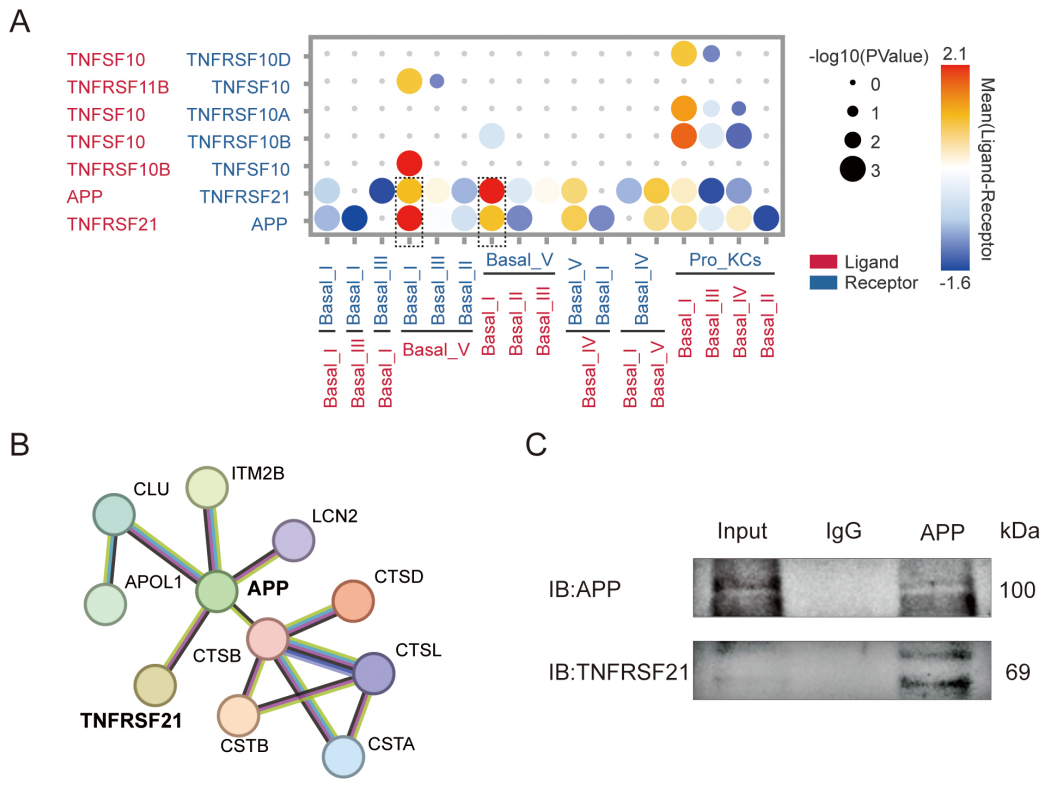

Fig. 4. Interaction of TNFRSF21 and amyloid precursor protein (APP) during keratinization. (A) Protein–protein interaction (PPI) analysis revealed that TNFRSF21 and APP undergo significant interaction. The dashed box highlights that APP and TNFRSF21 have the strongest PPI within the TNFRSF family. (B) This interaction was further validated using the String database. (C) Western blot analysis confirmed the interaction between TNFRSF21 and APP in human oral keratinocytes (HOKs) cells.

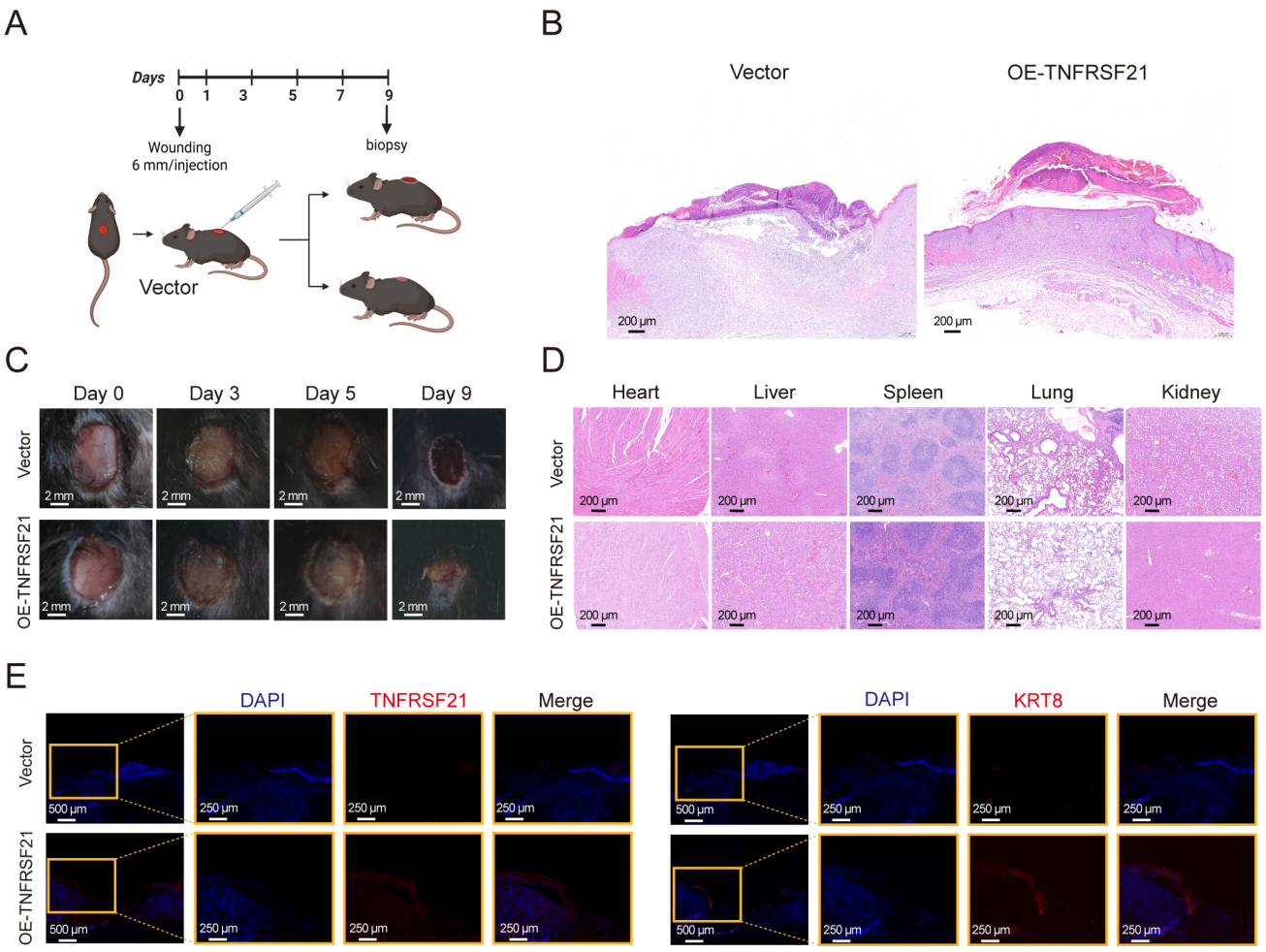

Fig. 5. Overexpression of TNFRSF21 promotes keratinized wound healing in mouse dorsal skin. (A) Diagram of the experimental design used to evaluate skin wound healing in C57BL/6 mice. On day 0, a 6-mm full-thickness skin incision was created using a biopsy punch as the wound model, followed by the injection of either empty vector or overexpression plasmids into the wound site. (B) Representative hematoxylin and eosin (H&E)-stained skin sections on day 9 after the injection of empty vector or overexpression plasmid. Scale bar = 200 μm. (C) Photographs of the wound area in C57BL/6 mice treated with either an empty vector or an overexpression plasmid on days 0, 3, 5, and 9 during the wound healing process. Scale bar = 2 mm. (D) Representative H&E-stained sections of the heart, liver, spleen, lung, and kidney on day 9 after injection with empty vector or overexpression plasmid. Scale bar = 200 μm. (E) Skin sections stained by immunofluorescence on day 9 after injection of empty vector or overexpression plasmid. The field of view is 5×, scale bar = 500 μm. The yellow boxes are enlarged views. The field of view is 10×, scale bar = 250 μm.

conditions, including diabetes and cardiovascular diseases [32,33]. The gingival epithelium serves as a critical protective barrier against pathogens and toxins [34]. Bacterial toxins and inflammatory cytokines such as TNF-α can disrupt tight junctions between gingival epithelial cells, including Claudin-1 and adherens junctions. This loosens the connections between cells, thereby increasing cell permeability and further exacerbating the destruction of gingival epithelial cells [10,35]. However, the mechanisms driving aberrant epithelial keratinization in periodontitis remain poorly understood. The present research identified *TNFRSF21* as a pivotal modulator of impaired keratinization in the periodontal epithelium. When combined with *APP*, *TNFRSF21* promotes the expression of KRTs. During PDT, *TNFRSF21* promotes tight junctions (e.g., *Claudin-1*) and adherens junctions, thereby protecting the epithelial barrier and promoting epithelial repair. We also developed an *in vitro* keratinization gradient model, offering a new strategy for studying periodontal keratinization loss. Therefore, *TNFRSF21* appears to play a dual critical role in periodontitis by orchestrating repair of the epithelial barrier through regulation of keratinization and stabilizing intercellular junctions. This not only addresses a significant gap in our understanding of the mechanism underlying aberrant epithelial keratinization in periodontitis, but also identifies a novel molecular target for therapeutic strategies targeting dysfunction of the epithelial barrier.

In the initial stage of periodontitis, the plaque biofilm activates the host immune response, leading to the production of reactive oxygen species (ROS), which then attack biological macromolecules such as proteins, lipids, and DNA [36]. Furthermore, ROS impairs fibroblasts, reduces collagen synthesis, and activates matrix metalloproteinases (MMPs), resulting in degradation of the extracellular matrix [36]. Previous studies have reported a marked expansion of the *TNFRSF21*$^{+}$ fibroblast population during the progression of periodontitis, leading to neutrophil infiltration [20,37]. These fibroblasts secrete chemokines and cytokines such as C-X-C Motif Chemokine Ligand 1, which intensify inflammation in periodontal tissues and can also regulate osteocyte activity, affecting the metabolic balance and regeneration of periodontal bone [20]. In addition, the excessive accumulation of neutrophils in periodontitis may compromise the keratinization and barrier function of the gingival epithelium, which could in turn intensify the inflammatory response [6]. Similar to our study, previous research has shown that *TNFRSF11A* (also known as *RANK*) can significantly promote the proliferation and survival of thymic epithelial cells, thereby enhancing thymic regeneration through activation of the *RANK-RANKL* signaling pathway [38]. However, our study is the first to demonstrate that *TNFRSF21* modulates keratin expression by HOK cells as periodontitis evolves. Moreover, we found that *TNFRSF21* interacts with *APP*, with this interaction being particularly evident in PPI analysis of scRNA-seq data.

Previous research on *APP* has predominantly focused on its role in the onset and progression of Alzheimer's disease (AD) [39]. Accumulating evidence indicates that periodontitis may indirectly aggravate AD pathology by enhancing systemic inflammation and disrupting intestinal homeostasis [40,41]. In AD, *APP* is cleaved by β-secretase to generate N-terminal fragment of *APP*, which binds to Death Receptor 6 (*DR6*) and activates caspase-6, thereby contributing to neurodegeneration [42]. In contrast, studies on skin wound repair have shown that *APP* promotes the proliferation, differentiation, and migration of keratinocytes, suggesting a potential regulatory role in keratin expression [43,44]. Notably, the *APP* fragment involved in epithelial repair is thought to be sAPPα (soluble amyloid precursor protein alpha), which is produced by α-secretase cleavage [45,46]. In *APP/APLP2* (Amyloid Precursor-Like Protein 2) double-knockout keratinocytes, the impaired proliferation, adhesion, and migration of these cells can be rescued by exogenous sAPPα, thus providing direct evidence of its importance in maintaining the repair phenotype and supporting wound re-epithelialization [45]. Our study is the first to identify an interaction between *TNFRSF21* and *APP* in human oral keratinocytes. This interaction appears to enhance keratin protein expression and may contribute to periodontal tissue repair, likely through the α-secretase–derived sAPPα fragment. Future investigations are warranted to further delineate the mechanism by which distinct *APP* fragments regulate epithelial repair. This groundbreaking discovery deepens our understanding of the biological functions of TNFRSF members and further delineates their influence on periodontal diseases, providing a novel perspective in periodontitis research.

5. Conclusion

The current findings demonstrate that *TNFRSF21* enhances wound healing during periodontitis treatment via the regulation of keratinization and tight junction integrity in oral epithelial cells. This potentially occurs through the involvement of α-secretase-derived sAPPα fragments in upregulating keratin expression. Our discovery provides a foundation for developing novel therapeutic strategies that target epithelial dysfunction in keratinization-related disorders.

Availability of Data and Materials

The accession number of the single-cell RNA-seq reported in this paper comes from the Gene Expression Omnibus (GEO): GSE171213 (https://www.ncbi.nlm.nih.gov/geo/query/acc.cgi?acc=GSE171213). Data supporting the results of this study can be provided at the reasonable request of the corresponding author.

Author Contributions

Software, Investigation, Writing—original draft preparation: WZ, YZ, SJ. Writing—review and editing: HZ, WZ, WS, MW. Visualization: ZS, BL, FX, YL, YY. Supervision: HZ, WS, MW. Conceptualization, Funding acquisition: HZ, MW, WS. All authors contributed to editorial changes in the manuscript. All authors read and approved the final manuscript. All authors have participated sufficiently in the work and agreed to be accountable for all aspects of the work.

Ethics Approval and Consent to Participate

All animal work was performed in accordance with the ARRIVE guidelines 2.0. The animal research project was approved by the Ethical Committee at Anhui Medical University on May 30, 2023, with the approval number LLSC20232087. Human Gingival Tissue Collection: Gingival tissues were collected from healthy volunteers or chronic periodontitis patients undergoing implant surgery at College & Hospital of Stomatology, Anhui Medical University. All subjects or their legal guardians signed an informed-consent form permitting the use of surplus surgical tissue for research. This study has been approved by College & Hospital of Stomatology, Anhui Medical University (Approval Number: T2021014). The study was carried out in accordance with the guidelines of the Declaration of Helsinki.

Acknowledgment

We thank Yi Zhang for providing technical assistance in single-cell RNA-Seq analysis.

Funding

This work was supported by the 2023 Disciplinary Construction Project in the School of Dentistry, Anhui Medical University (2023xkfyts01), the Key Project of Natural Science Research in Anhui Provincial Universities (2024AH050683).

Conflict of Interest

The authors declare no conflict of interest.

Supplementary Material

Supplementary material associated with this article can be found, in the online version, at https://doi.org/10.31083/FBL48371.

References

[1] Easter QT, Fernandes Matuck B, Beldorati Stark G, Worth CL, Predeus AV, Fremin B, *et al*. Single-cell and spatially resolved interactomics of tooth-associated keratinocytes in periodontitis. Nature Communications. 2024; 15: 5016. https://doi.org/10.1038/s41467-024-49037-y.

[2] Holtfreter B, Conrad E, Kocher T, Baumeister SE, Völzke H, Welk A. Interdental cleaning aids are beneficial for oral health at 7-year follow-up: Results from the Study of Health in Pomerania (SHIP-TREND). Journal of Clinical Periodontology. 2024; 51: 252–264. https://doi.org/10.1111/jcpe.13936.

[3] Chapple ILC, Hirschfeld J, Cockwell P, Dietrich T, Sharma P. Interplay between periodontitis and chronic kidney disease. Nature Reviews. Nephrology. 2025; 21: 226–240. https://doi.org/10.1038/s41581-024-00910-5.

[4] Wang C, Zhao Q, Chen C, Li J, Zhang J, Qu S, *et al*. CD301b^{+} macrophage: the new booster for activating bone regeneration in periodontitis treatment. International Journal of Oral Science. 2023; 15: 19. https://doi.org/10.1038/s41368-023-00225-4.

[5] Bosshardt DD. The periodontal pocket: pathogenesis, histopathology and consequences. Periodontology 2000. 2018; 76: 43–50. https://doi.org/10.1111/prd.12153.

[6] Cui YY, Yang YH, Zheng JY, Ma HH, Han X, Liao CS, *et al*. Elevated neutrophil extracellular trap levels in periodontitis: Implications for keratinization and barrier function in gingival epithelium. Journal of Clinical Periodontology. 2024; 51: 1210–1221. https://doi.org/10.1111/jcpe.14025.

[7] Vaernewyck V, Arzi B, Sanders NN, Cox E, Devriendt B. Mucosal Vaccination Against Periodontal Disease: Current Status and Opportunities. Frontiers in Immunology. 2021; 12: 768397. https://doi.org/10.3389/fimmu.2021.768397.

[8] Rocco S, Tempesta AA, Aluisio GV, Mezzatesta ML, Romano A, Schiavo V, *et al*. Antibacterial and cytotoxic effects of chlorhexidine combined with sodium DNA on oral microorganisms: an *in vitro* study using*Dictyostelium discoideum*. Journal of Oral Microbiology. 2025; 17: 2595797. https://doi.org/10.1080/20002297.2025.2595797.

[9] Iglesias-Bartolome R, Uchiyama A, Molinolo AA, Abusleme L, Brooks SR, Callejas-Valera JL, *et al*. Transcriptional signature primes human oral mucosa for rapid wound healing. Science Translational Medicine. 2018; 10: eaap8798. https://doi.org/10.1126/scitranslmed.aap8798.

[10] Groeger S, Meyle J. Oral Mucosal Epithelial Cells. Frontiers in Immunology. 2019; 10: 208. https://doi.org/10.3389/fimmu.2019.00208.

[11] Watts TH, Yeung KKM, Yu T, Lee S, Eshraghisamani R. TNF/TNFR Superfamily Members in Costimulation of T Cell Responses-Revisited. Annual Review of Immunology. 2025; 43: 113–142. https://doi.org/10.1146/annurev-immunol-082423-040557.

[12] Dostert C, Grusdat M, Letellier E, Brenner D. The TNF Family of Ligands and Receptors: Communication Modules in the Immune System and Beyond. Physiological Reviews. 2019; 99: 115–160. https://doi.org/10.1152/physrev.00045.2017.

[13] Thapa B, Kato S, Nishizaki D, Miyashita H, Lee S, Nesline MK, *et al*. OX40/OX40 ligand and its role in precision immune oncology. Cancer Metastasis Reviews. 2024; 43: 1001–1013. https://doi.org/10.1007/s10555-024-10184-9.

[14] Jeong D, Kim HS, Kim HY, Kang MJ, Jung H, Oh Y, *et al*. Soluble Fas ligand drives autoantibody-induced arthritis by binding to DR5/TRAIL-R2. eLife. 2021; 10: e48840. https://doi.org/10.7554/eLife.48840.

[15] Ababneh O, Nishizaki D, Kato S, Kurzrock R. Tumor necrosis factor superfamily signaling: life and death in cancer. Cancer Metastasis Reviews. 2024; 43: 1137–1163. https://doi.org/10.1007/s10555-024-10206-6.

[16] Medler J, Nelke J, Weisenberger D, Steinfatt T, Rothaug M, Berr S, *et al*. TNFRSF receptor-specific antibody fusion proteins with targeting controlled FcγR-independent agonistic activity. Cell Death & Disease. 2019; 10: 224. https://doi.org/10.1038/s41419-019-1456-x.

[17] Remedios KA, Zirak B, Sandoval PM, Lowe MM, Boda D, Henley E, *et al*. The TNFRSF members CD27 and OX40 coordinately limit T_H17 differentiation in regulatory T cells. Science Immunology. 2018; 3: eaau2042. https://doi.org/10.1126/sciimmunol.aau2042.

[18] Gao X, Zhou J, Qiao Y, Lin C, Zhang G, Wu Q, *et al*. ATP6V0A4 as a novel prognostic biomarker and potential therapeutic target in oral squamous cell carcinoma. BMC Oral Health. 2025; 25: 1269. https://doi.org/10.1186/s12903-025-06653-4.

[19] Munk A, Philippi V, Buchecker V, Bankstahl M, Glasenapp A, Blutke A, *et al*. Refining pain management in mice by comparing multimodal analgesia and NSAID monotherapy for neurosurgical procedures. Scientific Reports. 2024; 14: 18691. https://doi.org/10.1038/s41598-024-69075-2.

[20] Chen Y, Wang H, Yang Q, Zhao W, Chen Y, Ni Q, *et al*. Single-cell RNA landscape of the osteoimmunology microenvironment in periodontitis. Theranostics. 2022; 12: 1074–1096. https://doi.org/10.7150/thno.65694.

[21] Huang LJ, Mao XT, Li YY, Liu DD, Fan KQ, Liu RB, *et al*. Multiomics analyses reveal a critical role of selenium in controlling T cell differentiation in Crohn's disease. Immunity. 2021; 54: 1728–1744.e1727. https://doi.org/10.1016/j.immuni.2021.07.004.

[22] Miao X, Huang Y, Ge KX, Xu Y. Application of scRNA-seq in Dental Research: Seeking Regenerative Clues From the Structure of Tooth and Periodontium in Physical or Pathological States. Frontiers in Bioscience (Landmark edition). 2025; 30: 26200. https://doi.org/10.31083/FBL26200.

[23] Hu Y, Wan S, Luo Y, Li Y, Wu T, Deng W, *et al*. Benchmarking algorithms for single-cell multi-omics prediction and integration. Nature Methods. 2024; 21: 2182–2194. https://doi.org/10.1038/s41592-024-02429-w.

[24] Korsunsky I, Millard N, Fan J, Slowikowski K, Zhang F, Wei K, *et al*. Fast, sensitive and accurate integration of single-cell data with Harmony. Nature Methods. 2019; 16: 1289–1296. https://doi.org/10.1038/s41592-019-0619-0.

[25] Kobak D, Berens P. The art of using t-SNE for single-cell tran-

scriptomics. Nature Communications. 2019; 10: 5416. https://doi.org/10.1038/s41467-019-13056-x.
[26] Troulé K, Petryszak R, Cakir B, Cranley J, Harasty A, Prete M, *et al*. CellPhoneDB v5: inferring cell-cell communication from single-cell multiomics data. Nature Protocols. 2025; 20: 3412–3440. https://doi.org/10.1038/s41596-024-01137-1.
[27] Dobin A, Davis CA, Schlesinger F, Drenkow J, Zaleski C, Jha S, *et al*. STAR: ultrafast universal RNA-seq aligner. Bioinformatics (Oxford, England). 2013; 29: 15–21. https://doi.org/10.1093/bioinformatics/bts635.
[28] Xu S, Hu E, Cai Y, Xie Z, Luo X, Zhan L, *et al*. Using clusterProfiler to characterize multiomics data. Nature Protocols. 2024; 19: 3292–3320. https://doi.org/10.1038/s41596-024-01020-z.
[29] Zhou S, Chen J, Cao R. Association between retinol intake and periodontal health in US adults. BMC Oral Health. 2023; 23: 61. https://doi.org/10.1186/s12903-023-02761-1.
[30] Pondeljak N, Lugović-Mihić L, Tomić L, Parać E, Pedić L, Lazić-Mosler E. Key Factors in the Complex and Coordinated Network of Skin Keratinization: Their Significance and Involvement in Common Skin Conditions. International Journal of Molecular Sciences. 2023; 25: 236. https://doi.org/10.3390/ijms25010236.
[31] Yang Z, Yu M, Li X, Tu Y, Wang C, Lei W, *et al*. Retinoic acid inhibits the angiogenesis of human embryonic stem cell-derived endothelial cells by activating FBP1-mediated gluconeogenesis. Stem Cell Research & Therapy. 2022; 13: 239. https://doi.org/10.1186/s13287-022-02908-x.
[32] Kapila YL. Oral health's inextricable connection to systemic health: Special populations bring to bear multimodal relationships and factors connecting periodontal disease to systemic diseases and conditions. Periodontology 2000. 2021; 87: 11–16. https://doi.org/10.1111/prd.12398.
[33] Ganesan SM, Vazana S, Stuhr S. Waistline to the gumline: Relationship between obesity and periodontal disease-biological and management considerations. Periodontology 2000. 2021; 87: 299–314. https://doi.org/10.1111/prd.12390.
[34] Lee JS, Yilmaz Ö. Key Elements of Gingival Epithelial Homeostasis upon Bacterial Interaction. Journal of Dental Research. 2021; 100: 333–340. https://doi.org/10.1177/0022034520973012.
[35] Groeger SE, Meyle J. Epithelial barrier and oral bacterial infection. Periodontology 2000. 2015; 69: 46–67. https://doi.org/10.1111/prd.12094.
[36] Sczepanik FSC, Grossi ML, Casati M, Goldberg M, Glogauer M, Fine N, *et al*. Periodontitis is an inflammatory disease of oxidative stress: We should treat it that way. Periodontology 2000. 2020; 84: 45–68. https://doi.org/10.1111/prd.12342.
[37] Cai C, Guan L, Wang C, Hu R, Ou L, Jiang Q. The role of fibroblast-neutrophil crosstalk in the pathogenesis of inflammatory diseases: a multi-tissue perspective. Frontiers in Immunology. 2025; 16: 1588667. https://doi.org/10.3389/fimmu.2025.1588667.
[38] Irla M. RANK Signaling in the Differentiation and Regeneration of Thymic Epithelial Cells. Frontiers in Immunology. 2021; 11: 623265. https://doi.org/10.3389/fimmu.2020.623265.
[39] Tian Q, Li J, Wu B, Pang Y, He W, Xiao Q, *et al*. APP lysine 612 lactylation ameliorates amyloid pathology and memory decline in Alzheimer's disease. The Journal of Clinical Investigation. 2025; 135: e184656. https://doi.org/10.1172/JCI184656.
[40] Chen H, Liao Y, Zhang X, Shen H, Shang D, He Z, *et al*. Age- and sex-related differences of periodontal bone resorption, cognitive function, and immune state in APP/PS1 murine model of Alzheimer's disease. Journal of Neuroinflammation. 2023; 20: 153. https://doi.org/10.1186/s12974-023-02790-1.
[41] Hao X, Li Z, Li W, Katz J, Michalek SM, Barnum SR, *et al*. Periodontal Infection Aggravates C1q-Mediated Microglial Activation and Synapse Pruning in Alzheimer's Mice. Frontiers in Immunology. 2022; 13: 816640. https://doi.org/10.3389/fimmu.2022.816640.
[42] Chen X, Jiang XM, Zhao LJ, Sun LL, Yan ML, Tian Y, *et al*. MicroRNA-195 prevents dendritic degeneration and neuron death in rats following chronic brain hypoperfusion. Cell Death & Disease. 2017; 8: e2850. https://doi.org/10.1038/cddis.2017.243.
[43] Kummer C, Wehner S, Quast T, Werner S, Herzog V. Expression and potential function of beta-amyloid precursor proteins during cutaneous wound repair. Experimental Cell Research. 2002; 280: 222–232. https://doi.org/10.1006/excr.2002.5631.
[44] Li Y, Wang Y, Zhang W, Jiang L, Zhou W, Liu Z, *et al*. Overexpression of Amyloid Precursor Protein Promotes the Onset of Seborrhoeic Keratosis and is Related to Skin Ageing. Acta Dermato-venereologica. 2018; 98: 594–600. https://doi.org/10.2340/00015555-2911.
[45] Smith J, Rai V. Novel Factors Regulating Proliferation, Migration, and Differentiation of Fibroblasts, Keratinocytes, and Vascular Smooth Muscle Cells during Wound Healing. Biomedicines. 2024; 12: 1939. https://doi.org/10.3390/biomedicines12091939.
[46] Harris SS, Wolf F, De Strooper B, Busche MA. Tipping the Scales: Peptide-Dependent Dysregulation of Neural Circuit Dynamics in Alzheimer's Disease. Neuron. 2020; 107: 417–435. https://doi.org/10.1016/j.neuron.2020.06.005.